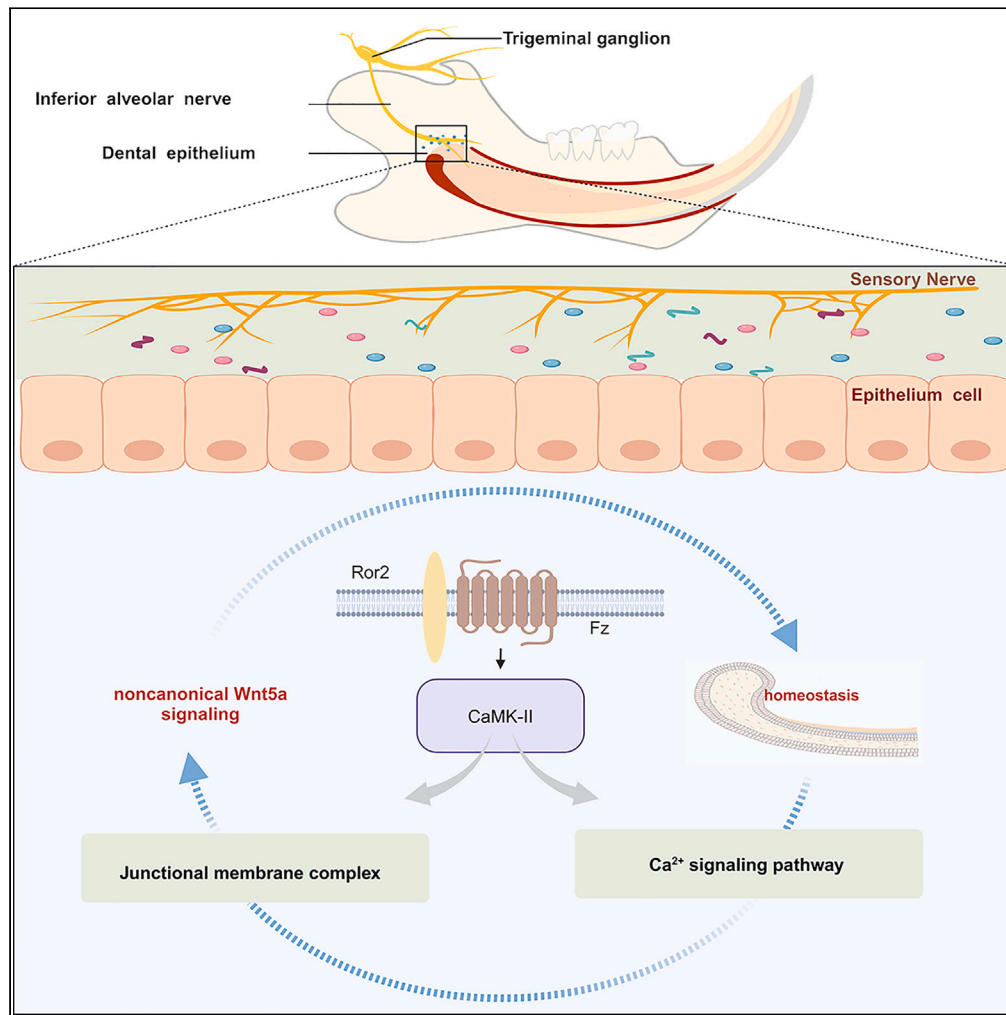


Article

The sensory nerve regulates stem cell homeostasis through Wnt5a signaling



Ting Zhang,
Jiaying Liu, Weiqiu
Jin, ..., Shaoyun
Jiang, Yin Xiao,
Fuhua Yan

jiangshaoyun11@126.com (S.J.)
yin.xiao@griffith.edu.au (Y.X.)
yanfh@nju.edu.cn (F.Y.)

Highlights

IAN is essential in stem cell homeostasis for enamel mineralization and development

IAN primarily regulates dental epithelial stem cells through sensory nerves

Sensory nerves affect enamel development by regulating the expression of Wnt5a

Zhang et al., iScience 27,
111035
October 18, 2024 © 2024 The
Author(s). Published by Elsevier
Inc.
[https://doi.org/10.1016/
j.isci.2024.111035](https://doi.org/10.1016/j.isci.2024.111035)



Article

The sensory nerve regulates stem cell homeostasis through Wnt5a signaling

Ting Zhang,^{1,5} Jiaying Liu,^{1,2,5} Weiqiu Jin,^{1,5} Hua Nie,¹ Sheng Chen,¹ Xuna Tang,¹ Rong Liu,³ Min Wang,¹ Rixin Chen,¹ Jiangyue Lu,¹ Jun Bao,¹ Shaoyun Jiang,^{4,*} Yin Xiao,^{2,*} and Fuhua Yan^{1,6,*}

SUMMARY

Increasing evidence indicates that nerves play a significant role in regulating stem cell homeostasis and developmental processes. To explore the impact of nerves on epithelial stem cell homeostasis during tooth development, the regulation of sensory nerves on stem cell homeostasis was investigated using a rat model of incisor development. Impaired mineralization, decreased enamel thickness, and fractured enamel rods of the incisor were observed after denervation. qPCR and histological staining revealed that the expression of enamel-related factors ameloblastin (AMBN), kallikrein-4, amelogenin (Amelx), collagen type XVII (col17a), and enamelin were decreased in the incisor enamel of rats with sensory nerve injury. The decreased expression of Wnt5a in ameloblasts was coupled with the downregulation of calcium ion-related calmodulin kinase II. These results implicate that the sensory nerves are essential in stem cell homeostasis for enamel mineralization and development.

INTRODUCTION

Stem cells play a crucial role throughout the entire process of organism development. The stem cell niches refer to the microenvironment that maintains their stemness. Precise control over stem cell differentiation and tissue structure is crucial for organogenesis, development, and tissue homeostasis.¹ However, studying the niche remains challenging due to the intricate regulatory networks and dynamic changes of the stem cell niche.

The constant self-renewal and replenishment of epithelial and mesenchymal stem cell populations in rodent incisors provides an ideal model to study dynamic stem cell niches² for stem cell generation, differentiation, and homeostasis. Enamel formation is a complex process by which stem cells in the cervical loop region differentiate and proliferate into new ameloblasts, which is known to be affected by various signaling pathways, including Wnt,³ sonic hedgehog (SHH),⁴ bone morphogenetic proteins (BMP),^{5,6} and Notch.^{7,8} The maturation of enamel matrix involves various enamel formation proteins such as amelogenin x-linked (AMELX), enamelin (ENAM),⁹ and ameloblastin (AMBN),¹⁰ as well as proteases like metalloproteinase-20 (MMP20) and kallikrein-4 (KLK4), and factors for cell adhesion including collagen XVII (COL17a), amelotin (AMTN), and odontogenic ameloblast-associated protein (ODAM).¹¹

In recent years, extensive research has shown that nerves are a crucial part of the stem cell niche, indispensable for tooth and periodontal tissue regeneration.¹² Numerous mesenchymal stem cells derived from peripheral nerve-related glial cells are involved in the development, self-renewal, and repair processes of teeth.¹³ Additionally, high calcitonin gene-related peptide α (CGRP α) expression was found in the epithelial condensed cells between the enamel depression and the epithelial surface layer of the tooth bud at E14.5, indicating that CGRP α may be related to the formation of the tooth germ.¹⁴ Scholars have not only studied the anatomical relationship between nerves and the tooth germ or enamel organs but have also investigated the impact of nerves on tooth development using denervation models.^{15–18} Moreover, sensory nerve injury can lead to the dysfunction of dental pulp stem cells induced by the activin B/SMAD2/3 signaling pathway *in vitro*.¹⁷ The Chai et al. also found that sensory nerves are crucial for maintaining mesenchymal tissue homeostasis and the continuous proliferation of mesenchymal stromal cells (MSCs) in adult mouse incisors.¹⁵ Shh produced by neurons activates Gli1⁺ expression in mesenchymal cells around the cervical loop, affecting the stability and repair of MSCs in the incisors.¹⁵ Denervation results in hard tissue defects in teeth and disrupts the development of incisors. Recent studies have discovered that fibroblast growth factor 1 (FGF1), a ligand secreted by sensory nerves, directly regulates MSCs in the incisor by binding to FGFR1 and activates the FGF/p-JNK/mTOR/autophagy axis to maintain tissue homeostasis.¹⁶

¹Nanjing Stomatological Hospital, Affiliated Hospital of Medical School, Institute of Stomatology, Nanjing University, Nanjing, China

²School of Medicine and Dentistry, Griffith University, Gold Coast, QLD 4222, Australia

³Department of Periodontology, Guiyang Hospital of Stomatology, Guiyang 550002, GuiZhou, China

⁴Stomatological Center, Peking University Shenzhen Hospital, Guangdong Provincial High-level Clinical Key Specialty, Shenzhen Clinical Research Center for Oral Diseases, Guangdong Province Engineering Research Center of Oral Disease Diagnosis and Treatment, Shenzhen 5180036, Guangdong, China

⁵These authors contributed equally

⁶Lead contact

*Correspondence: jiangshaoyun11@126.com (S.J.), yin.xiao@griffith.edu.au (Y.X.), yanfh@nju.edu.cn (F.Y.)
<https://doi.org/10.1016/j.isci.2024.111035>



However, the role of nerves in the stem cell niche and their involvement in regulating enamel formation and development remain largely unknown. The mechanism by which nerves regulate stem cell homeostasis and how the enamel structure changes after denervation are also still being determined. Therefore, in the present study, we used rat incisor enamel development as a model to investigate the role of nerves in stem cell homeostasis. The research performed surgical denervation and chemical sensory nerve loss to elucidate the impact of nerves on enamel development and explore the molecular mechanisms regulating enamel development. This study aimed to provide a theoretical basis for understanding how nerves affect stem cell homeostasis and potentially contribute to future tissue regeneration.

RESULTS

Impaired incisor mineralization in rats after nerve damage

The inferior alveolar nerve is a mixed nerve that is composed of general somatic sensory fibers and special visceral motor fibers. To further clarify whether the sensory nerve was responsible for this change, we established a rat model of sensory nerve damage by capsaicin injection (Figure 1A) and an inferior alveolar nerve injury model (Figure 1B). To confirm the effectiveness of the model, we observed the expression of the nerve and sensory nerve markers using the axon marker protein gene product 9.5 (PGP 9.5) and the sensory nerve-specific marker CGRP, respectively. Three weeks after denervation, the decrease in PGP 9.5 and CGRP expression in the inferior alveolar nerve (IAN) and capsaicin groups confirmed the successful establishment of the model (Figure 1C). The incisors on the surgically denervated side were chalky white. The incisors in the capsaicin group did not change in color, but yellow-white opaque patches were observed on the tips of the incisors (Figure 2B). The micro-CT results showed that the thickness of enamel in the IAN and capsaicin groups significantly decreased compared to the sham-operated group. Additionally, mineral deposition was significantly delayed and enamel formation was reduced (Figures 2A and 2D). Scanning electron microscopy revealed that compared with the sham-operated group, the IAN group did not have clearly defined enamel rod structures in the enamel, with visible gaps between intertwined enamel rods, without clear boundaries and collapse. Under high magnification, the enamel rods appeared to be fractured, resembling strands of hair falling off the enamel rods with a loose structure (Figure 2C). Furthermore, as shown in Figure 2E, the hardness of enamel with nerve loss was significantly reduced.

Denervation inhibits epithelium-derived enamel regeneration in rats

To clarify the changes in the differentiation process of dental epithelial cells after denervation, longitudinal sections of incisors were examined. Dental epithelial cells in the cervical loop were indistinguishable among three groups (Figure 3B). During the secretion and maturation stages of enamel development, there is no apparent change in the morphology of the ameloblasts. In contrast, visible empty vesicles were observed between the ameloblasts during the secretion stages in the IAN and capsaicin groups (Figure 3B). According to Masson staining, the onset of enamel matrix deposition from the cervical loop of the incisors moved distally to the labial cervical loop after denervation (Figures 3C and 3E). Additionally, labeling ameloblasts with Amelx revealed reduced secretion in both the IAN and capsaicin groups, indicating a weakened enamel generation ability (Figures 3D and 3F). Hard tissue sections were used to further elaborate on the differences in the enamel generated after denervation without decalcification. The enamel rod structure was more pronounced in the IAN group, with an increased number of organic structures such as enamel tufts (Figure 3G). These findings suggest inadequate mineralization in the incisor teeth following loss of the inferior alveolar nerve.

Denervation disrupted the development of enamel

Transcriptomic analysis was conducted in the cervical loop area in the IAN and sham-operated groups, to investigate the effects of nerve damage on stem cells and enamel changes at the molecular level. Based on the analysis of differentially expressed genes, we found that 23 genes were upregulated and 47 genes were downregulated (Figure 4A). The transcriptomic analysis of cervical loop in rats with inferior alveolar nerve loss and sham-operated group also revealed that genes related to enamel development, such as ODAM, AMTN, and kallikrein-related peptidase 4 (KLK4), were significantly downregulated in the IAN group. Furthermore, the expression of genes associated with epithelial-mesenchymal interactions, such as COL17a, laminin subunit gamma 3 (LAMC3), and claudin 11 (CLDN11), also significantly decreased after nerve loss, all of which are crucial for enamel formation (Figure 4B).¹⁹ Kyoto encyclopedia of genes and genomes (KEGG) enrichment analysis showed that nerve loss affected calcium signaling pathways (Figure 4D). In contrast, the gene ontology (GO) analysis indicated that the downregulated genes were enriched in the junction membrane complex (Figure 4E). The downregulation of these genes may explain the tissue defects between ameloblasts and enamel epithelium after nerve loss. Meanwhile, the expression of KLK4, an enzyme involved in enamel development, decreased after denervation by immunofluorescence detection (Figures 4F and 4G). The qPCR results further confirmed that the expression of genes related to enamel development, such as AMBN, Amelx, COL17a, ENAM, and KLK4, were significantly downregulated after denervation (Figure 4H). Additionally, the expression of Wnt5a was downregulated (Figure 4C), indicating that the nerve may affect enamel development possibly through its association with Wnt5a.

Sensory nerves affect the homeostasis of rat incisors via the wnt5a signaling pathway

To investigate the regulatory role of Wnt5a in epithelial stem cells after denervation, immunofluorescence staining of rat incisors was performed. The results revealed that the expression level of Wnt5a in the sham-operated group was significantly higher than in the other groups (Figures 5A–5D and 5I). Additionally, immunohistochemical staining of the Wnt5a-related receptor Ror2 revealed no significant differences in expression among the groups (Figures 5B–5E and 5I). Subsequently, we stained for the critical factor CaMK-II in the Wnt5a-Ca²⁺

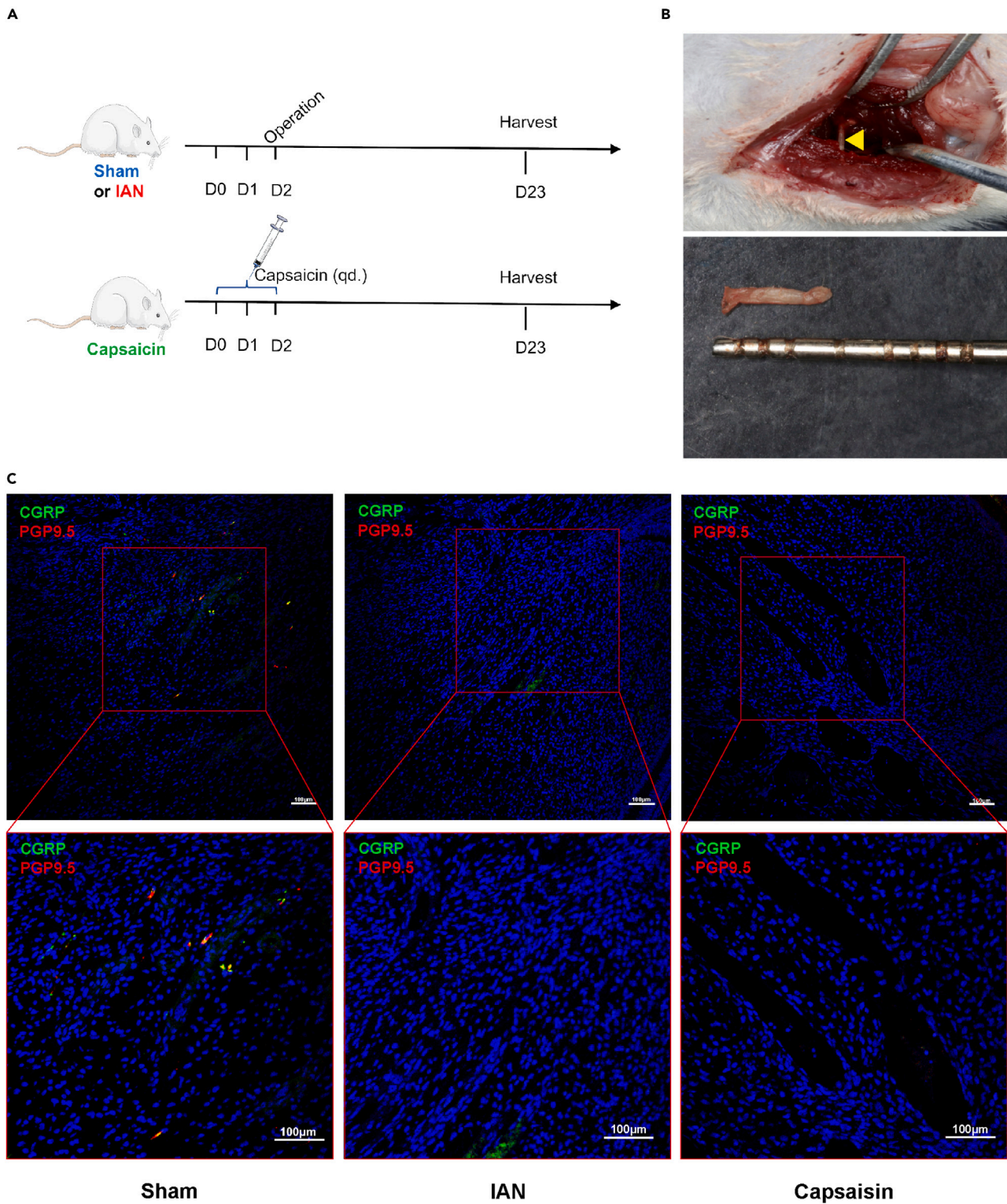


Figure 1. Establishment of a model for rats with nerve injury

(A) Design of the experiment.

(B) Surgical diagram of the inferior alveolar nerve injury model. The yellow arrows indicate the inferior alveolar nerve of rat.

(C) After 21 days of denervation, the IAN and capsaicin groups showed decreased expression of PGP 9.5 and CGRP.

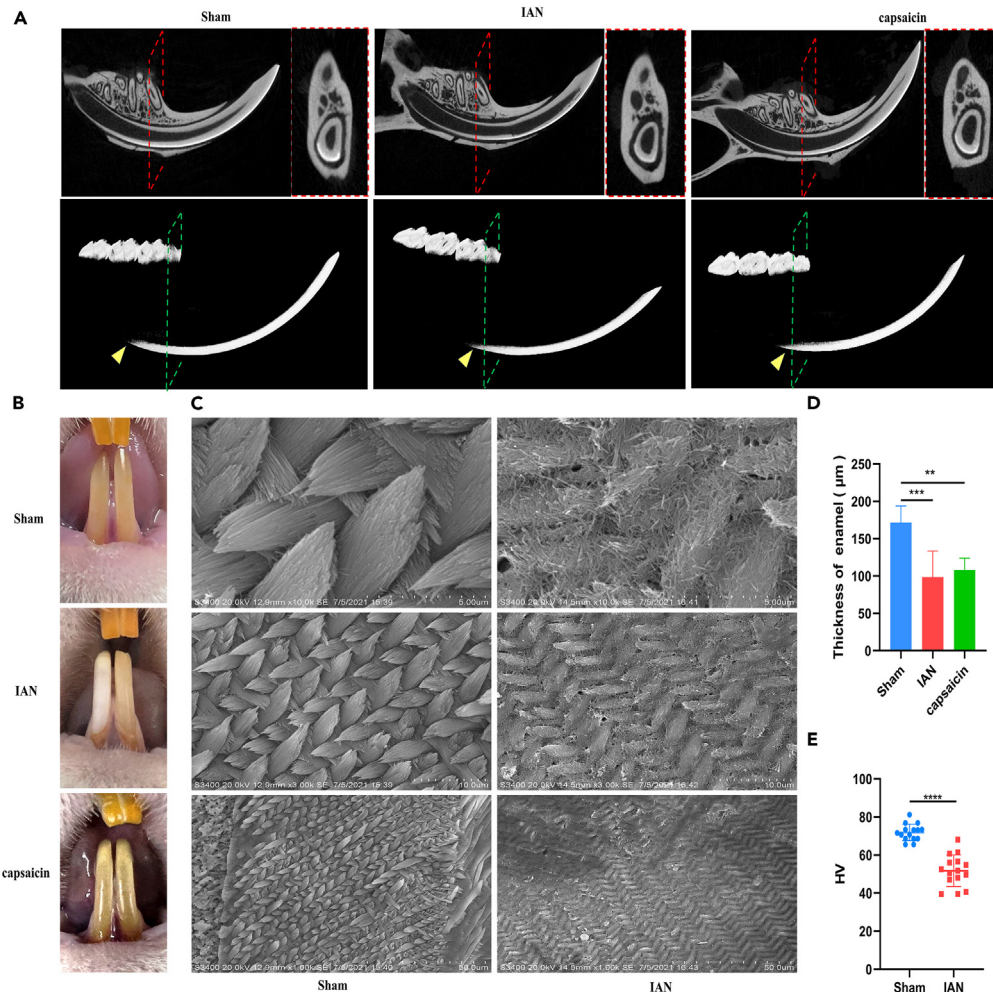


Figure 2. Impaired mineralization of incisors in rats after nerve damage

(A) Micro-computed tomography showed that the enamel thickness of the IAN and capsaicin groups were significantly thinner than that of the sham-operated group. Mineral deposition was delayed, and enamel formation was reduced. The yellow arrows indicate the beginning of the rat's incisor tooth enamel (IAN, inferior alveolar nerve).

(B) In the IAN group, the denervated incisors appeared chalky white. In the capsaicin group, but yellow-white opaque areas could be observed at the tips of the incisors (IAN, inferior alveolar nerve).

(C) Scanning electron microscopy results showed that compared to the sham-operated group, the enamel in the IAN group had no distinct enamel prism structure, with visible gaps between crossed enamel prisms, no clear boundaries, and collapsed enamel prisms. At high magnification, the enamel prisms appeared fragmented and separated (IAN, inferior alveolar nerve).

(D) Quantification of the thickness of enamel between the groups ($n = 6$ per group, mean \pm SD. ** $p < 0.01$, *** $p < 0.001$, one-way ANOVA, IAN, inferior alveolar nerve).

(E) Vickers hardness results revealed a significant decrease in enamel hardness in rats after inferior alveolar nerve loss ($n = n = 3$ to 6 per group, mean \pm SD. **** $p < 0.0001$, Unpaired t test, IAN, inferior alveolar nerve).

pathway and found that its expression decreased significantly after denervation. Interestingly, CaMK-II expression was higher in the capsaicin group than in the IAN group (Figures 5C and 5F). We hypothesized that after inferior alveolar nerve loss, other signaling pathways might further inhibit the calcium signaling pathway, which may explain the more severe mineral loss observed in the incisors of the IAN group compared to the capsaicin group by naked eye observation. β -catenin is a critical factor in the classical Wnt pathway, and studies have shown that Wnt5a antagonizes the Wnt/ β -catenin pathway.²⁰ Immunohistochemical staining revealed an increase in β -catenin expression after nerve loss, suggesting that denervation inhibits Wnt5a and promotes β -catenin expression (Figures 5G and 5H). Meanwhile, the gene expression levels in each group showed a similar trend to the histological staining results (Figure 5I). Furthermore, the qPCR results indicated that the expression levels of the classic wnt/ β -catenin pathway-related gene wnt3a were upregulated in the capsaicin and IAN groups (Figure 5I). Therefore, these data suggest that the sensory nerves may impair rat incisor development by affecting the non-classical Wnt5a- Ca^{2+} pathway.

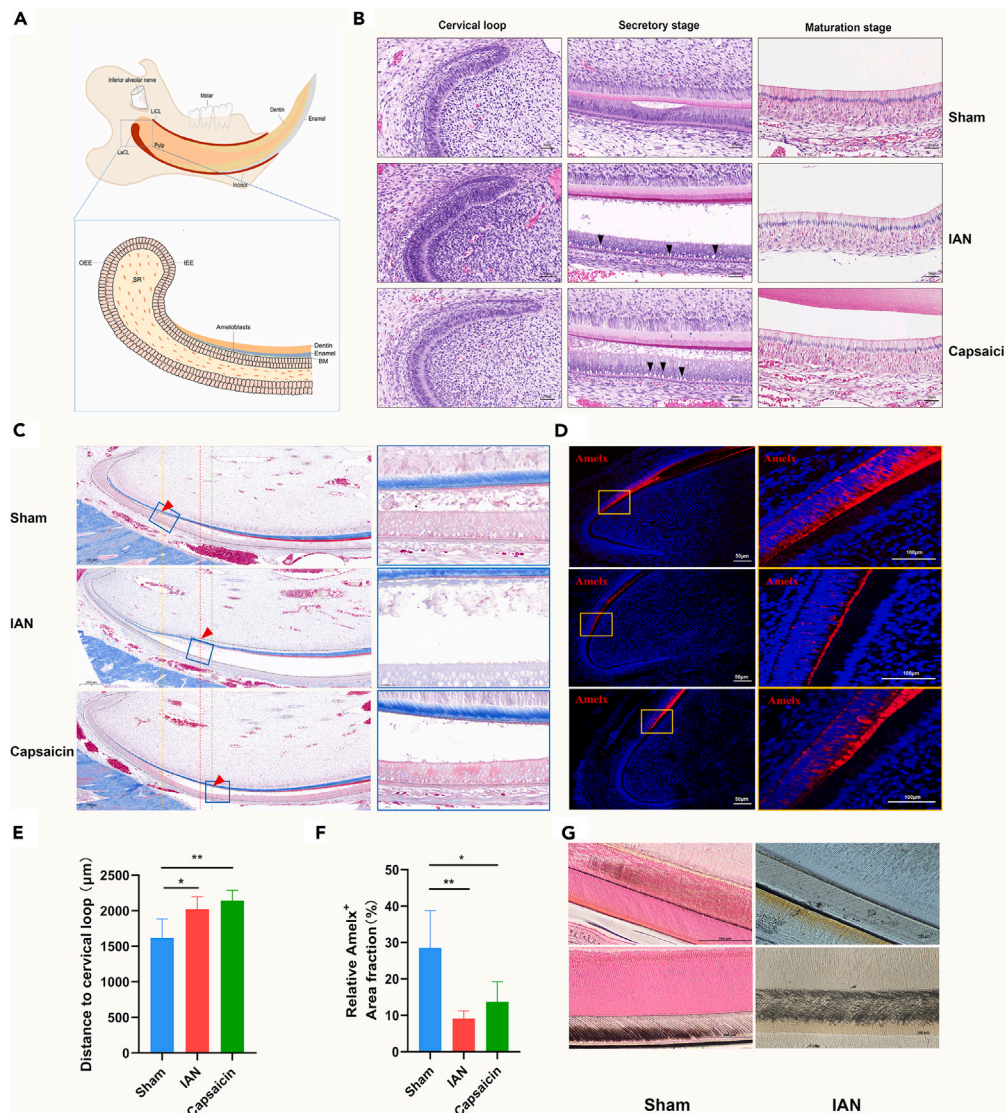


Figure 3. Denervation inhibits epithelium-derived enamel regeneration in rats

(A) Schematic illustration of the dental epithelium of rat mandibular incisors. (IAN, inferior alveolar nerve; BM, basal membrane; IEE, inter enamel epithelium; LaCL, labial cervical loop; LiCL, lingual cervical loop; OEE, outer enamel epithelium; SR, stellate reticular layer).

(B) Hematoxylin and eosin (HE) stained sections revealed the presence of vacuolated gaps between ameloblasts and enamel matrix cells in the secretory stages of amelogenesis. The black arrows indicate vacuolated gaps between the ameloblasts and enamel matrix cells (IAN, inferior alveolar nerve).

(C) Masson's trichrome staining (MTS) showed delayed enamel deposition in the far-middle region of the incisor in the IAN and capsaicin groups, with enamel matrix deposition moving posteriorly after denervation (where dentin stained blue and enamel stained red). The red arrows indicate the starting position of the enamel in the incisor tooth (IAN, inferior alveolar nerve).

(D) Immunofluorescence staining with amelogenin (Amelx) showed reduced secretion of Amelx in the IAN and capsaicin groups (IAN, inferior alveolar nerve).

(E) The distance of the starting position of the enamel to cervical loop in each group ($n = 5$ per group, mean \pm SD. $*p < 0.05$, one-way ANOVA, IAN, inferior alveolar nerve).

(F) Quantification of Amelx positive area between the groups ($n = 4$ per group, mean \pm SD. $*p < 0.05$, $**p < 0.01$, one-way ANOVA, IAN, inferior alveolar nerve).

(G) Hard tissue sections revealed a more pronounced enamel rod structure under the microscope in IAN group, as well as an increase in organic structures such as enamel tufts.

DISCUSSION

Owing to the presence of epithelial and mesenchymal stem cells including ameloblasts, odontoblasts, and cementoblasts, the incisors of rodents can grow continuously throughout their lifespan, thus replacing lost tissue caused by wear or injury.² Ameloblast progenitor cells are essential epithelial stem cells in tooth development, capable of forming new enamel to maintain the growth of rodent incisors. Our

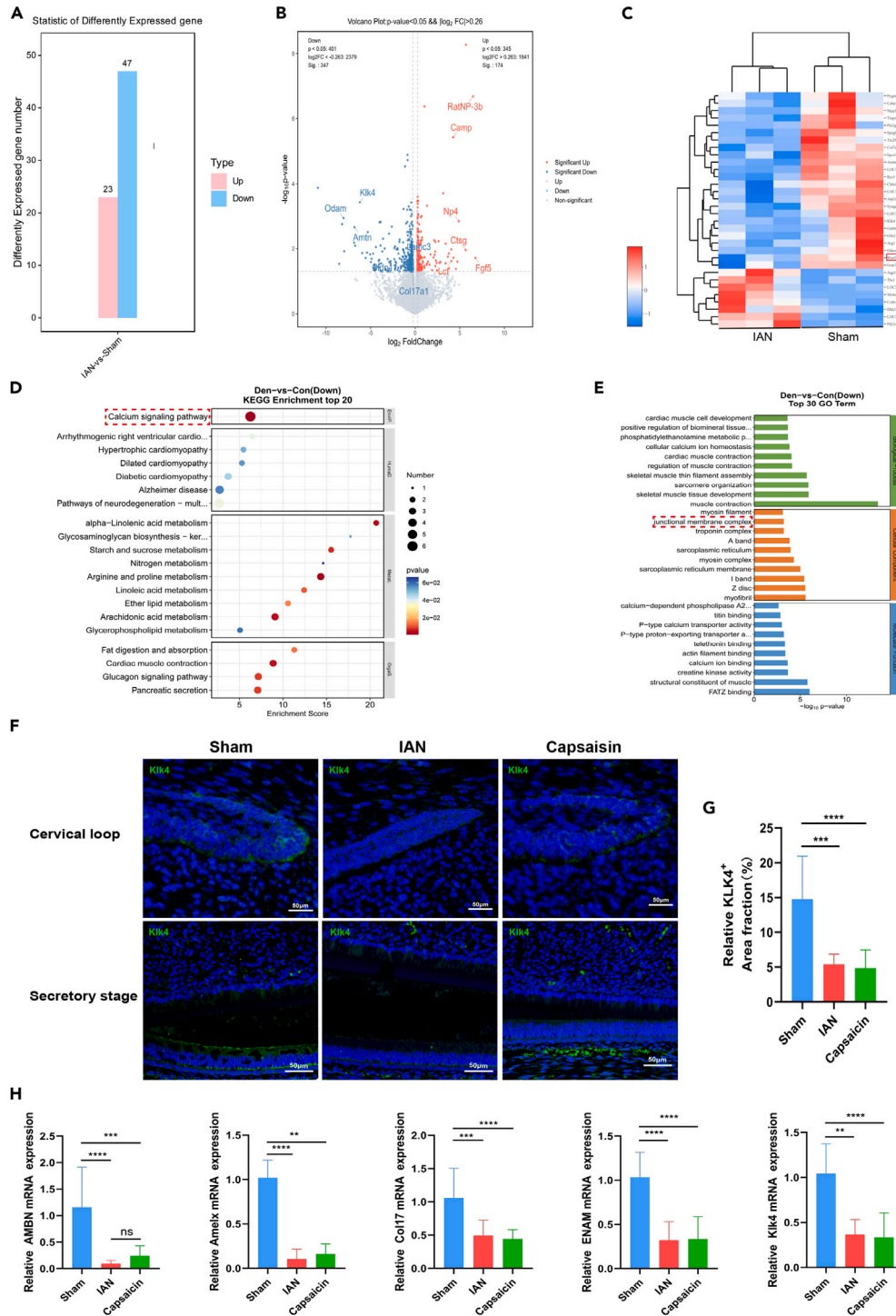


Figure 4. Denervation disrupted the development of enamel

(A) Transcriptomic analysis of the cervical loop region in rats without inferior alveolar nerve revealed 23 upregulated genes and 47 downregulated genes. (B) Transcriptomic analysis identified significant downregulation of enamel development-associated genes ODAM, KLK4, and AMTN, as well as genes associated with cell junction, such as COL17a, LAMC3, and CLDN11, in the IAN group. (C) Transcriptomic analysis showed downregulation of the *wnt5a* gene in the IAN group. (D) KEGG enrichment analysis revealed that nerve ligation affects the calcium signaling pathway. (E) GO analysis indicated that downregulated genes in the nerve ligation group are enriched in the junctional membrane complex.

Figure 4. Continued

(F and G) Immunofluorescence staining showed that the expression of the enzyme KLK4 related to enamel development decreased after denervation ($n = 4$ to 6 per group, mean \pm SD. **** $p < 0.0001$. one-way ANOVA, IAN, inferior alveolar nerve).

(H) The expression of genes in the cervical loop region was verified by qPCR, and the expression of enamel-related genes AMBN, Amelx, Col17a, ENAM, and KLK4 decreased after denervation ($n = 4$ to 6 per group, mean \pm SD. ns, no statistical significance, ** $p < 0.01$, *** $p < 0.001$, **** $p < 0.0001$. Kruskal-Wallis test, IAN, inferior alveolar nerve).

research revealed that sensory nerves are essential components of the stem cell niche in the incisors of adult rats and can influence enamel development by affecting ameloblasts.

Enamel formation involves complex physiological processes that are tightly regulated by critical genes and spatiotemporal programming. Alterations in the conditions of enamel development can result in changes in the quantity, composition, and structure of the tissue.²¹ Our experiments demonstrated that denervation in rats not only inhibited the thickness and length of dental enamel but also altered the structure of enamel, affecting enamel hardness and mineralization. Amelx is a hallmark protein of enamel matrix cells,²² playing a significant role in maintaining enamel structure and crystal growth. After denervation, the expression of Amelx decreases, indicating a weakened ability of enamel matrix formation by ameloblasts. Masson staining and micro-CT also confirmed delayed and reduced enamel matrix deposition after denervation. Meanwhile, the transcriptomic and qPCR results in the cervical loop area showed a decrease in the expression of the enamel-related genes AMBN, ENAM, ODAM, and AMTN. Both ODAM and AMTN are members of the secretory calcium-binding phosphoprotein (SCPP) gene family, which are expressed in the basement membranes of transitional and mature ameloblast, influencing the attachment between mature ameloblasts and mineralized enamel.²³ The incisor enamel of AMTN^{-/-} mice appears chalky white, with enamel matrix retention and delayed mineralization, and the surface enamel is soft and easily peels off.²⁴ Knockout mice for ODAM exhibit structural changes in the attachment epithelium and cannot adhere to the surfaces of healthy teeth.²⁵ ENAM is the largest enamel matrix protein (EMP), and ENAM mutation can lead to proteinopathy, resulting in insufficient mineralization and hardness of mature stage enamel.²⁶ AMBN is a multifunctional extracellular matrix protein that is involved in cell signaling and polarity, cell adhesion to the developing enamel matrix, and maintenance of prismatic enamel morphology.²⁷ AMBN mutation can also cause enamel hypoplasia.²⁸ Therefore, the decreased expression of these genes after sensory nerve loss may contribute to the amelogenesis imperfecta of enamel in rat incisors. In addition, the enamel-epithelium junction is an essential part of enamel formation, and detachment of ameloblasts from enamel can lead to developmental enamel defects. The gene sequencing results revealed a decrease in the expression of COL17a, LAMC3, and CLDN11, which are associated with epithelial-mesenchymal interactions. GO analysis revealed downregulation of expression in the junctional membrane complex. H&E staining also revealed the presence of vacuolar gaps between ameloblasts during the secretion stages after the loss of the inferior alveolar nerve and sensory nerve, which may be associated with disrupted cell junctions. These findings suggest that disruption of cell junction-related factors in epithelial stem cells may contribute to enamel mineralization defects after denervation. KLK4 is a glycosylated serine protease resembling pancreatic trypsinogen. It helps to remove protein degradation fragments from cells and increases the width and thickness of enamel crystals. This is crucial for removal of enamel proteins and maturation of enamel crystals.²⁹ KLK4^{-/-} mice have normal enamel thickness after tooth eruption but quickly wear off or crack within the enamel layer above the dentin-enamel junction. The maturation of enamel prisms and interprismatic crystals is delayed, resulting in protein accumulation. The enamel crystals fail to interlock with each other to grow as a cohesive entity but rather break away from the fractured enamel, resembling strands of hair falling off the rods.³⁰ This phenomenon is consistent with the scanning electron microscope results for the IAN group. Furthermore, a decrease in KLK4 expression was observed at the genetic and protein level after the loss of the inferior alveolar nerve and sensory nerve. This result explains the changes observed in the ameloblasts of rats after nerve loss under an electron microscope. These findings suggest that the loss of sensory nerves can alter the expression of KLK4 in ameloblasts, thereby further influencing enamel maturation.

Numerous scholars have discovered that the nervous system, especially the sensory nerves, is dominant in regulating stem cell maintenance and tissue homeostasis.³¹ Cao's group found that sensory nerves regulate MSC differentiation in the bone marrow of adult mice via the PGE2/EP4 axis.^{32,33} Studies have also shown that sensory nerves may play a role in the stem cell niche of hair follicle melanocytes.³⁴⁻³⁶ To study the ideal objects for the stem cell niche, the incisors of rodents were considered. The expression of CD90-positive stem cells decreased in incisors after IAN removal.¹⁸ Meanwhile, Cai and Xuan also discovered that sensory nerves influence tooth development and enamel formation by affecting mesenchymal stem cells.¹⁵⁻¹⁷ Therefore, in this study, we aimed to further investigate whether the inferior alveolar nerve, as a mixed nerve, primarily affects the homeostasis of rat incisor stem cells through sensory nerves. In addition, we explored the effects of sensory nerves on the homeostasis of epithelial stem cells. This experiment showed that the IAN and capsaicin groups of rats exhibited similar characteristics, suggesting that the inferior alveolar nerve primarily affects the homeostasis of rat incisor stem cells through sensory nerves, potentially through the influence of ameloblasts.

Multiple signaling pathways play essential roles in the growth and homeostasis of adult mouse incisors. The Wnt/ β -catenin signaling pathway plays a crucial role in the development of tooth germ, the formation of dental tissue, and tooth eruption.^{37,38} Compared to the classical Wnt/ β -catenin signaling pathway, the non-classical Wnt pathway has received less attention. Wnt5a is the most crucial protein that mediates the non-classical Wnt signaling pathway and regulates cellular functions such as proliferation, differentiation, migration, adhesion, and polarity.^{39,40} Wnt5a is expressed in both dental epithelium and mesenchyme during tooth development.⁴¹ Transcriptome sequencing of the IAN and sham-operated groups revealed that the expression of Wnt5a, but not that of other Wnt family members, was significantly decreased. We hypothesized that the nervous system might affect the homeostasis of rat incisors through the Wnt5a signaling pathway. Furthermore, both immunofluorescence staining and qPCR results revealed a significant decrease in Wnt5a expression in ameloblasts of

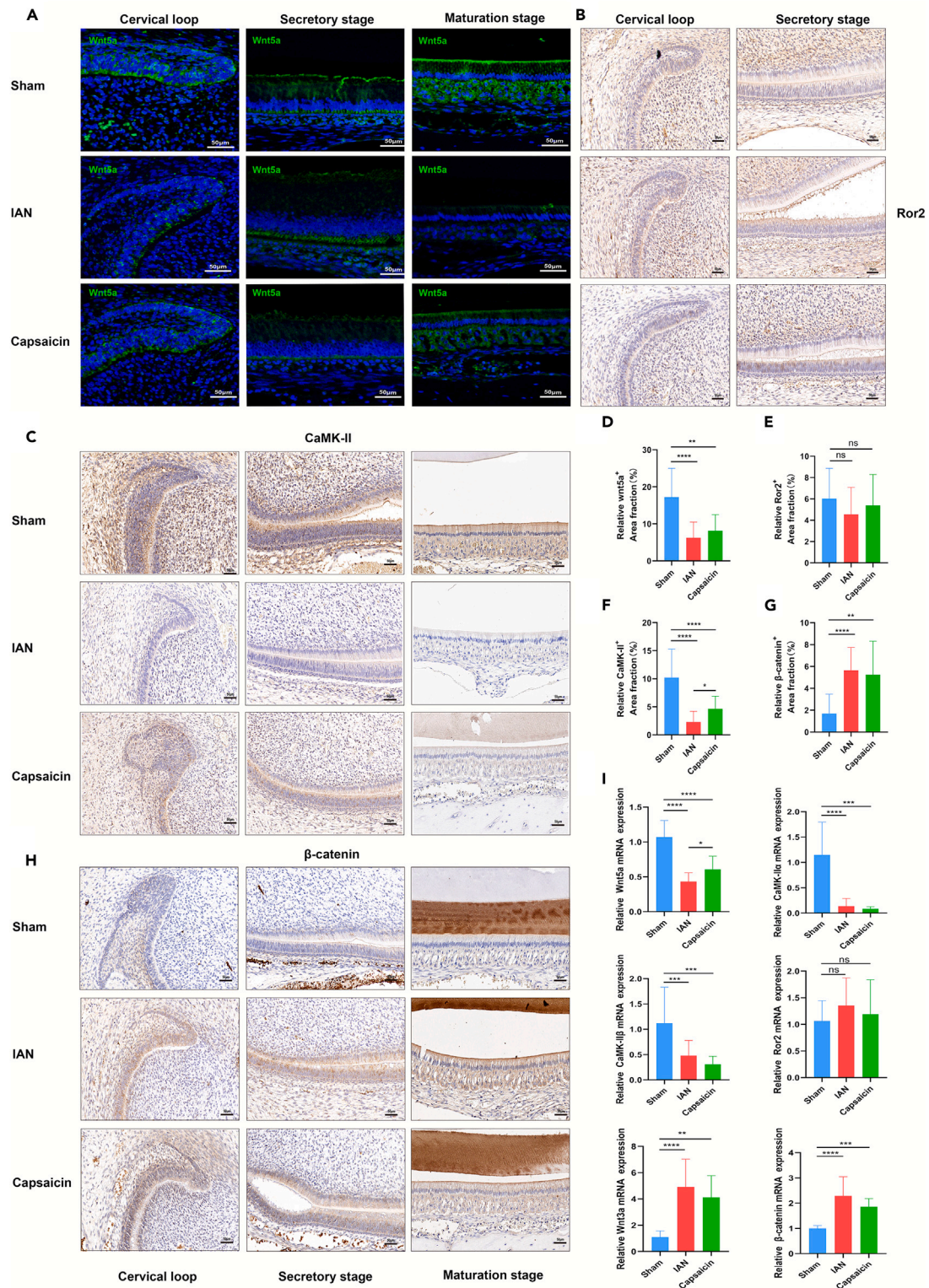


Figure 5. Sensory nerves affect the homeostasis of rat incisors via the wnt5a signaling pathway

(A) Immunofluorescence staining of rat incisors revealed that the expression level of wnt5a was significantly higher in the sham-operated group compared with other groups.

(B) Immunohistochemical examination showed no significant difference in the expression of the wnt5a receptor Ror2 among the different groups.

Figure 5. Continued

- (C) Immunohistochemical staining revealed a significant decrease in CaMK-II expression after denervation, but the expression of CaMK-II in the capsaicin group was higher than that in the IAN group.
- (D) Quantification of the expression of *wnt5a* in rat incisors ($n = 4$ to 6 per group, mean \pm SD. * $p < 0.05$, ** $p < 0.01$, Kruskal-Wallis test, IAN, inferior alveolar nerve).
- (E) Quantification of the expression of *Ror2* in rat incisors ($n = 6$ per group, mean \pm SD. ns, no statistical significance, one-way ANOVA, IAN, inferior alveolar nerve).
- (F) Quantification of the expression of CaMK-II in rat incisors ($n = 6$ per group, mean \pm SD. * $p < 0.05$, **** $p < 0.0001$, one-way ANOVA, IAN, inferior alveolar nerve).
- (H) Immunohistochemical staining revealed an increase in β -catenin expression after denervation.
- (G) Quantification of the expression of β -catenin in rat incisors ($n = 4$ to 6 per group, mean \pm SD. ** $p < 0.01$, **** $p < 0.0001$, Kruskal-Wallis test, IAN, inferior alveolar nerve).
- (I) qPCR detection found that the non-classical Wnt signaling pathway-related genes *wnt5a*, *CaMK-II α* , and *CaMK-II β* had decreased expression after denervation, while the IAN group showed a further decrease in *wnt5a* gene expression compared to the capsaicin group. The expression levels of the classical Wnt/ β -catenin pathway-related genes *wnt3a* and β -catenin increased. Meanwhile, there was no significant difference in the expression levels of *wnt5a* receptor *Ror2* mRNA among the three groups ($n = 4$ to 6 per group, mean \pm SD. ns, no statistical significance, * $p < 0.05$, ** $p < 0.01$, *** $p < 0.001$, **** $p < 0.0001$, The differential expression of *wnt5a* mRNA was analyzed using one-way ANOVA, while the statistical analysis of the differential expression of the remaining mRNAs was conducted using the Kruskal-Wallis test, IAN, inferior alveolar nerve).

the IAN and capsaicin groups, suggesting that *Wnt5a* may be a critical regulatory molecule affecting the sensory nerve-mediated modulation of ameloblast. Our research group has previously discovered that *Wnt5a* regulates odontoblast differentiation and affects tooth development.⁴² It was also found that *Wnt5a/Ror2* can impact the interaction between mesenchymal stem cells and transit amplifying cells and influence the steady-state development of mouse incisors.⁴³ In this study, we found that the expression of the *Ror2* receptor did not undergo significant changes after denervation. This suggests that nerves may only alter the expression of *Wnt5a* but have no effect on the expression of *Ror2* receptors. In addition, we found through KEGG analysis that the expression of the calcium signaling pathway decreases after denervation. The *Wnt5a/Ca²⁺* signaling pathway is also an essential component of the non-canonical Wnt signaling pathway. We speculate that the downregulation of *Wnt5a* expression after denervation may have further effects on calcium ion channels and consequently affect enamel development. Immunohistochemical staining and the expression of mRNA showed that the expression of CaMK-II was significantly reduced after denervation, which may further affect calcium ion transporters. *Wnt5a*, an essential protein that mediates the non-canonical Wnt signaling pathway, can act synergistically or antagonistically with the canonical Wnt/ β -catenin pathway under certain conditions.²⁰ *Wnt5a* activates NLK or *Ror2* to downregulate the expression of β -catenin. It can also promote the degradation of β -catenin by activating *Siah2*.⁴⁴ Additionally, *Wnt5a* can inhibit the Wnt/ β -catenin pathway by competing with *Wnt3a* for Fz receptors.⁴⁵ However, further studies suggest that when Wnt receptors are excessive, *Wnt5a* synergistically enhances the Wnt/ β -catenin pathway. The impact of *Wnt5a* on the Wnt/ β -catenin pathway depends on factors such as receptor levels. In the two groups of rats with denervation, β -catenin expression increased as *Wnt5a* expression decreased, suggesting a mutual antagonism between *Wnt5a* and the Wnt/ β -catenin pathway. Therefore, sensory nerves primarily affect the calcium signaling pathway via *Wnt5a* and antagonize the canonical Wnt/ β -catenin pathway.

Conclusions

In summary, this study demonstrated that the inferior alveolar nerve, which is primarily a sensory nerve, can influence the homeostasis of rat incisors by directly regulating the expression of *Wnt5a* in dental epithelial stem cells. This finding validates the significance of sensory nerves in maintaining stem cell niches and their impact on tissue regeneration. It also provides the foundational knowledge for achieving temporally and functionally controlled regeneration. However, our understanding of neural regulation within stem cell niches in rodent incisors and other organs remains limited, and the complexity of these interactions in different microenvironments should be further elucidated in future studies.

Limitations of the study

This study only clarified the involvement of sensory nerves, particularly through *wnt5a* signaling, in influencing epithelial homeostasis of teeth and consequently affecting tooth development. However, the understanding of the regulatory factors of sensory nerves is still limited. Meanwhile, our understanding of neuronal regulation within stem cell niches in rodent incisors and other organs remains limited, and the complexity of these interactions in different microenvironments should be further elucidated in future studies.

RESOURCE AVAILABILITY**Lead contact**

Further information and requests for reagents should be directed to and will be fulfilled by the Lead Contact, Fuhua Yan (yanfh@nju.edu.cn).

Materials availability

This study did not generate new unique reagents. All stable reagents in this study are available from the [lead contact](#) with a completed material transfer agreement.

Data and code availability

- The sequence data reported in this paper have been deposited at the NCBI Sequence Read Archive (SRA) (BioProject ID: PRJNA1021553) and are publicly available as of the date of publication.
- This paper does not include original code.
- Any additional information needed to reanalyze the data is available from the [lead contact](#) upon reasonable request.

ACKNOWLEDGMENTS

This study was supported by National Key R&D Program of China (2022YFC2504200), Jiangsu Provincial Medical Key Discipline Cultivation Unit (JSDW202246), Jiangsu Province Key Research and Development Program (BE2022670), Nanjing Medical Science and Technique Development Foundation (YKK21185).

AUTHOR CONTRIBUTIONS

T.Z., J.L., and W.J. contributed to the conception, design, data acquisition, analysis, and interpretation, drafted, and revised the manuscript; S.C. contributed to tissue section staining. H.N., R.L., X.T., M.W., and J.B. contributed to data acquisition and interpretation and revised the manuscript; R.C. and J.L. contributed to data acquisition and analysis and revised the manuscript; F.Y., Y.X., and S. J. contributed to conception, design, data interpretation, and revised the manuscript. All authors read and approved the final manuscript.

DECLARATION OF INTERESTS

The authors declare no competing interests.

STAR★METHODS

Detailed methods are provided in the online version of this paper and include the following:

- [KEY RESOURCES TABLE](#)
- [EXPERIMENTAL MODEL AND STUDY PARTICIPANT DETAILS](#)
 - Animal administration
 - Establishment of a model for rats with loss of sensory nerve
 - Establishment of a model for rats with inferior alveolar nerve injury
- [METHOD DETAILS](#)
 - Histology and immunohistochemical analysis of incisor
 - Immunofluorescence analysis
 - Micro-computed tomography analysis
 - mRNA sequencing analysis
 - Hard tissue sectioning assay
 - Scanning electron microscopy
 - Vickers hardness testing
 - Quantitative real-time PCR (qPCR) of gene expression in the cervical loop region of rat incisors
- [QUANTIFICATION AND STATISTICAL ANALYSIS](#)

SUPPLEMENTAL INFORMATION

Supplemental information can be found online at <https://doi.org/10.1016/j.isci.2024.111035>.

Received: March 4, 2024

Revised: June 13, 2024

Accepted: September 23, 2024

Published: September 26, 2024

REFERENCES

1. Wang, X. (2019). Stem cells in tissues, organoids, and cancers. *Cell. Mol. Life Sci.* 76, 4043–4070. <https://doi.org/10.1007/s00018-019-03199-x>.
2. Krivanek, J., Soldatov, R.A., Kastriti, M.E., Chontorotzea, T., Herdina, A.N., Petersen, J., Szarowska, B., Landova, M., Matejova, V.K., Holla, L.I., et al. (2020). Dental cell type atlas reveals stem and differentiated cell types in mouse and human teeth. *Nat. Commun.* 11, 4816. <https://doi.org/10.1038/s41467-020-18512-7>.
3. Yu, T., and Klein, O.D. (2020). Molecular and cellular mechanisms of tooth development, homeostasis and repair. *Development* 147, dev184754. <https://doi.org/10.1242/dev.184754>.
4. Hosoya, A., Shalehin, N., Takebe, H., Shimo, T., and Irie, K. (2020). Sonic Hedgehog Signaling and Tooth Development. *Int. J. Mol. Sci.* 21, 1587. <https://doi.org/10.3390/ijms21051587>.
5. Murashima-Suginami, A., Kiso, H., Tokita, Y., Mihara, E., Nambu, Y., Uozumi, R., Tabata, Y., Bessho, K., Takagi, J., Sugai, M., and Takahashi, K. (2021). Anti-USAG-1 therapy for tooth regeneration through enhanced BMP signaling. *Sci. Adv.* 7, eabf1798. <https://doi.org/10.1126/sciadv.abf1798>.
6. Shi, C., Yuan, Y., Guo, Y., Jing, J., Ho, T.V., Han, X., Li, J., Feng, J., and Chai, Y. (2019). BMP Signaling in Regulating Mesenchymal Stem Cells in Incisor Homeostasis. *J. Dent. Res.* 98, 904–911. <https://doi.org/10.1177/0022034519850812>.
7. Jheon, A.H., Prochazkova, M., Meng, B., Wen, T., Lim, Y.J., Naveau, A., Espinoza, R., Cox, T.C., Sone, E.D., Ganss, B., et al. (2016). Inhibition of Notch Signaling During Mouse Incisor Renewal Leads to Enamel Defects. *J. Bone Miner. Res.* 31, 152–162. <https://doi.org/10.1002/jbmr.2591>.
8. Cai, X., Gong, P., Huang, Y., and Lin, Y. (2011). Notch signalling pathway in tooth development and adult dental cells. *Cell Prolif.* 44, 495–507. <https://doi.org/10.1111/j.1365-2184.2011.00780.x>.
9. Dong, C., Lamichhane, B., Yamazaki, H., Vasquez, B., Wang, J., Zhang, Y., Feng, J.Q., Margolis, H.C., Beniash, E., and Wang, X. (2022). The phosphorylation of serine(55) in enamel is essential for murine amelogenesis. *Matrix Biol.* 111, 245–263. <https://doi.org/10.1016/j.matbio.2022.07.001>.
10. Su, J., Bapat, R.A., Visakan, G., and Moradian-Oldak, J. (2022). Coemergence of the Amphipathic Helix on Ameloblastin With

- Mammalian Prismatic Enamel. *Mol. Biol. Evol.* 39, msac205. <https://doi.org/10.1093/molbev/msac205>.
11. Smith, C.E.L., Poulter, J.A., Antanaviciute, A., Kirkham, J., Brookes, S.J., Inglehearn, C.F., and Mighell, A.J. (2017). Amelogenesis Imperfecta; Genes, Proteins, and Pathways. *Front. Physiol.* 8, 435. <https://doi.org/10.3389/fphys.2017.00435>.
 12. Duan, Y., Liang, Y., Yang, F., and Ma, Y. (2022). Neural Regulations in Tooth Development and Tooth-Periodontium Complex Homeostasis: A Literature Review. *Int. J. Mol. Sci.* 23, 14150. <https://doi.org/10.3390/ijms232214150>.
 13. Kaukua, N., Shahidi, M.K., Konstantinidou, C., Dyachuk, V., Kaucka, M., Furlan, A., An, Z., Wang, L., Hultman, I., Ahrlund-Richter, L., et al. (2014). Glial origin of mesenchymal stem cells in a tooth model system. *Nature* 513, 551–554. <https://doi.org/10.1038/nature13536>.
 14. Maeda, Y., Miwa, Y., and Sato, I. (2019). Distribution of the neuropeptide calcitonin gene-related peptide-alpha of tooth germ during formation of the mouse mandible. *Ann. Anat.* 221, 38–47. <https://doi.org/10.1016/j.aanat.2018.09.001>.
 15. Zhao, H., Feng, J., Seidel, K., Shi, S., Klein, O., Sharpe, P., and Chai, Y. (2014). Secretion of shh by a neurovascular bundle niche supports mesenchymal stem cell homeostasis in the adult mouse incisor. *Cell Stem Cell* 14, 160–173. <https://doi.org/10.1016/j.stem.2013.12.013>.
 16. Pei, F., Ma, L., Jing, J., Feng, J., Yuan, Y., Guo, T., Han, X., Ho, T.V., Lei, J., He, J., et al. (2023). Sensory nerve niche regulates mesenchymal stem cell homeostasis via FGF/mTOR/autophagy axis. *Nat. Commun.* 14, 344. <https://doi.org/10.1038/s41467-023-35977-4>.
 17. Liu, A.Q., Zhang, L.S., Fei, D.D., Guo, H., Wu, M.L., Liu, J., He, X.N., Zhang, Y.J., Xuan, K., and Li, B. (2020). Sensory nerve-deficient microenvironment impairs tooth homeostasis by inducing apoptosis of dental pulp stem cells. *Cell Prolif.* 53, e12803. <https://doi.org/10.1111/cpr.12803>.
 18. Hayano, S., Fukui, Y., Kawanabe, N., Kono, K., Nakamura, M., Ishihara, Y., and Kamioka, H. (2018). Role of the Inferior Alveolar Nerve in Rodent Lower Incisor Stem Cells. *J. Dent. Res.* 97, 954–961. <https://doi.org/10.1177/0022034518758244>.
 19. Simmer, J.P., Hu, J.C.C., Hu, Y., Zhang, S., Liang, T., Wang, S.K., Kim, J.W., Yamakoshi, Y., Chun, Y.H., Bartlett, J.D., and Smith, C.E. (2021). A genetic model for the secretory stage of dental enamel formation. *J. Struct. Biol.* 213, 107805. <https://doi.org/10.1016/j.jsb.2021.107805>.
 20. Kikuchi, A., Yamamoto, H., Sato, A., and Matsumoto, S. (2012). Wnt5a: its signalling, functions and implication in diseases. *Acta Physiol.* 204, 17–33. <https://doi.org/10.1111/j.1748-1716.2011.02294.x>.
 21. Wright, J.T. (2023). Enamel Phenotypes: Genetic and Environmental Determinants. *Genes* 14, 545. <https://doi.org/10.3390/genes14030545>.
 22. Shemirani, R., Le, M.H., and Nakano, Y. (2023). Mutations Causing X-Linked Amelogenesis Imperfecta Alter miRNA Formation from Amelogenin Exon4. *J. Dent. Res.* 102, 1210–1219. <https://doi.org/10.1177/00220345231180572>.
 23. Fouillen, A., Dos Santos Neves, J., Mary, C., Castonguay, J.D., Moffatt, P., Baron, C., and Nanci, A. (2017). Interactions of AMTN, ODA1 and SCLPPQ1 proteins of a specialized basal lamina that attaches epithelial cells to tooth mineral. *Sci. Rep.* 7, 46683. <https://doi.org/10.1038/srep46683>.
 24. Nakayama, Y., Holcroft, J., and Ganss, B. (2015). Enamel Hypomineralization and Structural Defects in Amelotin-deficient Mice. *J. Dent. Res.* 94, 697–705. <https://doi.org/10.1177/0022034514566214>.
 25. Nishio, C., Wazen, R., Moffatt, P., and Nanci, A. (2013). Expression of odontogenic ameloblast-associated and amelotin proteins in the junctional epithelium. *Periodontology* 63, 59–66. <https://doi.org/10.1111/prd.12031>.
 26. Wang, Y.L., Lin, H.C., Liang, T., Lin, J.C.Y., Simmer, J.P., Hu, J.C.C., and Wang, S.K. (2024). ENAM Mutations Can Cause Hypomaturation Amelogenesis Imperfecta. *J. Dent. Res.* 103, 662–671. <https://doi.org/10.1177/00220345241236695>.
 27. Hany, U., Watson, C.M., Liu, L., Nikolopoulos, G., Smith, C.E.L., Poulter, J.A., Brown, C.J., Patel, A., Rodd, H.D., Balmer, R., et al. (2024). Novel Ameloblastin Variants, Contrasting Amelogenesis Imperfecta Phenotypes. *J. Dent. Res.* 103, 22–30. <https://doi.org/10.1177/00220345231203694>.
 28. Kegulian, N.C., Visakan, G., Bapat, R.A., and Moradian-Oldak, J. (2024). Ameloblastin and its multifunctionality in amelogenesis: a review. *Matrix Biol.* 131, 62–76. <https://doi.org/10.1016/j.matbio.2024.05.007>.
 29. Lacruz, R.S., Habelitz, S., Wright, J.T., and Paine, M.L. (2017). Dental Enamel Formation and Implications for Oral Health and Disease. *Physiol. Rev.* 97, 939–993. <https://doi.org/10.1152/physrev.00030.2016>.
 30. Simmer, J.P., Hu, Y., Lertlam, R., Yamakoshi, Y., and Hu, J.C.C. (2009). Hypomaturation enamel defects in *Klk4* knockout/*LacZ* knockin mice. *J. Biol. Chem.* 284, 19110–19121. <https://doi.org/10.1074/jbc.M109.013623>.
 31. Picoli, C.C., Costa, A.C., Rocha, B.G.S., Silva, W.N., Santos, G.S.P., Prazeres, P.H.D.M., Costa, P.A.C., Oropeza, A., da Silva, R.A., Azevedo, V.A.C., et al. (2021). Sensory nerves in the spotlight of the stem cell niche. *Stem Cells Transl. Med.* 10, 346–356. <https://doi.org/10.1002/sctm.20-0284>.
 32. Chen, H., Hu, B., Lv, X., Zhu, S., Zhen, G., Wan, M., Jain, A., Gao, B., Chai, Y., Yang, M., et al. (2019). Prostaglandin E2 mediates sensory nerve regulation of bone homeostasis. *Nat. Commun.* 10, 181. <https://doi.org/10.1038/s41467-018-08097-7>.
 33. Hu, B., Lv, X., Chen, H., Xue, P., Gao, B., Wang, X., Zhen, G., Crane, J.L., Pan, D., Liu, S., et al. (2020). Sensory nerves regulate mesenchymal stromal cell lineage commitment by tuning sympathetic tones. *J. Clin. Invest.* 130, 3483–3498. <https://doi.org/10.1172/JCI131554>.
 34. Hsu, Y.C., Li, L., and Fuchs, E. (2014). Emerging interactions between skin stem cells and their niches. *Nat. Med.* 20, 847–856. <https://doi.org/10.1038/nm.3643>.
 35. Zhang, B., Ma, S., Rachmin, I., He, M., Baral, P., Choi, S., Gonçalves, W.A., Shwartz, Y., Fast, E.M., Su, Y., et al. (2020). Hyperactivation of sympathetic nerves drives depletion of melanocyte stem cells. *Nature* 577, 676–681. <https://doi.org/10.1038/s41586-020-1935-3>.
 36. Riol-Blanco, L., Ordovas-Montanes, J., Perro, M., Naval, E., Thriot, A., Alvarez, D., Paust, S., Wood, J.N., and von Andrian, U.H. (2014). Nociceptive sensory neurons drive interleukin-23-mediated psoriasisform skin inflammation. *Nature* 510, 157–161. <https://doi.org/10.1038/nature13199>.
 37. Hermans, F., Hemeryck, L., Lambrichts, I., Bronckaers, A., and Vankelecom, H. (2021). Intertwined Signaling Pathways Governing Tooth Development: A Give-and-Take Between Canonical Wnt and Shh. *Front. Cell Dev. Biol.* 9, 758203. <https://doi.org/10.3389/fcell.2021.758203>.
 38. Lee, J.M., Qin, C., Chai, O.H., Lan, Y., Jiang, R., and Kwon, H.J.E. (2022). MSX1 Drives Tooth Morphogenesis Through Controlling Wnt Signaling Activity. *J. Dent. Res.* 101, 832–839. <https://doi.org/10.1177/00220345211070583>.
 39. Fu, Y., Wei, Y., Zhou, Y., Wu, H., Hong, Y., Long, C., Wang, J., Wu, Y., Wu, S., Shen, L., and Wei, G. (2021). Wnt5a Regulates Junctional Function of Sertoli cells Through PCP-mediated Effects on mTORC1 and mTORC2. *Endocrinology* 162, bqab149. <https://doi.org/10.1210/endoocr/bqab149>.
 40. Endo, M., Nishita, M., Fujii, M., and Minami, Y. (2015). Insight into the role of Wnt5a-induced signaling in normal and cancer cells. *Int. Rev. Cell Mol. Biol.* 314, 117–148. <https://doi.org/10.1016/bs.ircmb.2014.10.003>.
 41. Cai, J., Mutoh, N., Shin, J.-O., Tani-Ishii, N., Ohshima, H., Cho, S.-W., and Jung, H.-S. (2011). Wnt5a plays a crucial role in determining tooth size during murine tooth development. *Cell Tissue Res.* 345, 367–377. <https://doi.org/10.1007/s00441-011-1224-4>.
 42. Lin, M., Li, L., Liu, C., Liu, H., He, F., Yan, F., Zhang, Y., and Chen, Y. (2011). Wnt5a regulates growth, patterning, and odontoblast differentiation of developing mouse tooth. *Dev. Dyn.* 240, 432–440. <https://doi.org/10.1002/dvdy.22550>.
 43. Jing, J., Feng, J., Li, J., Zhao, H., Ho, T.V., He, J., Yuan, Y., Guo, T., Du, J., Urata, M., et al. (2021). Reciprocal interaction between mesenchymal stem cells and transit amplifying cells regulates tissue homeostasis. *Elife* 10, e59459. <https://doi.org/10.7554/eLife.59459>.
 44. Ren, D., Dai, Y., Yang, Q., Zhang, X., Guo, W., Ye, L., Huang, S., Chen, X., Lai, Y., Du, H., et al. (2019). Wnt5a induces and maintains prostate cancer cells dormancy in bone. *J. Exp. Med.* 216, 428–449. <https://doi.org/10.1084/jem.20180661>.
 45. Sato, A., Yamamoto, H., Sakane, H., Koyama, H., and Kikuchi, A. (2010). Wnt5a regulates distinct signalling pathways by binding to Frizzled2. *EMBO J.* 29, 41–54. <https://doi.org/10.1038/emboj.2009.322>.
 46. Ding, Y., Arai, M., Kondo, H., and Togari, A. (2010). Effects of capsaicin-induced sensory denervation on bone metabolism in adult rats. *Bone* 46, 1591–1596. <https://doi.org/10.1016/j.bone.2010.02.022>.
 47. Zhang, Z.K., Guo, X., Lao, J., and Qin, Y.X. (2017). Effect of capsaicin-sensitive sensory neurons on bone architecture and mechanical properties in the rat hindlimb suspension model. *J. Orthop. Translat.* 10, 12–17. <https://doi.org/10.1016/j.jot.2017.03.001>.

STAR★METHODS

KEY RESOURCES TABLE

REAGENT or RESOURCE	SOURCE	IDENTIFIER
Antibodies		
CGRP	Cell Signaling Technology	Cat#14959; RRID: AB_2798662
PGP9.5	Abcam	Cat#ab108986; RRID: AB_10891773
Almex	Affinity Biosciences	Cat#DF13729; RRID: AB_2846748
Wnt5a	Proteintech	Cat#55184-1-AP; RRID: AB_2881285
Klk4	LifeSpan Biosciences	Cat#LS-C335696-20; RRID: NA
Ror2	Abcam	Cat#ab190145; RRID: NA
CaMK-II	Abcam	Cat#ab134041; RRID: AB_2811181
β -catenin	Cell Signaling Technology	Cat#25362, RRID: AB_2798902
CoraLite488-conjugated Anti-Rabbit IgG(H + L)	Proteintech	Cat#RGAR002; RRID: AB_3073506
CoraLite594-conjugated Goat Anti-Mouse IgG	Proteintech	Cat#RGAM004; RRID: AB_3073502
CoraLite594-conjugated Goat Anti-Rabbit IgG(H + L)	Proteintech	Cat#SA00013-4; RRID: AB_2810984
Chemicals, peptides, and recombinant proteins		
capsaicin	Selleck	Cat#S1990
isoflurane	RWD	Cat#R510-22-10
EDTA, 0.5M	Corning	Cat#46-034-CI
TRIzol	Thermo Fisher Scientific	Cat#15596026
4'-6-diamidino-2-phenylindole	Abcam	Cat#ab104139
DAB Kit	MXB	Cat#1031
Pepsin Antigen Retrieval Kit	Sangon	Cat#E673007
Technovit 7200VLC	Kulzer	Cat#64709019
RNA Easy Fast Tissue Kit	TIANGEN	Cat# DP451
HiScript III RT SuperMix for qPCR	Vazyme	Cat# R323-01
PowerUp SYBR Green Master Mix	Thermo Fisher Scientific	Cat# A25742
Deposited data		
mRNA sequencing	In this study	SRA: PRJNA1021553
Experimental models: Organisms/strains		
Rat: CD(SD) IGS	Vital River Laboratory Animal Technology Co., Ltd.	Cat# 101
Software and algorithms		
PRISM	GraphPad Software	Version 8
ImageJ	NIH	https://imagej.nih.gov/ij/
Adobe Illustrator	Adobe	https://www.adobe.com/
BioRender	BioRender	https://www.biorender.com/
DESeq2 (1.22.2)	Bioconductor	https://bioconductor.org/packages/release/bioc/html/DESeq2.html

EXPERIMENTAL MODEL AND STUDY PARTICIPANT DETAILS

Animal administration

Adult Sprague–Dawley rats (male, 7 weeks old) were purchased from Charles River Laboratory, were raised under specific pathogen-free conditions with a 12-hour light/dark cycle. After a week of adaptation at the Animal Center of Nanjing Agricultural University, all rats were randomly subjected to the experiment. All experimental procedures were in accordance with the “Guide for the care and use of laboratory animals” and approved by the Animal Ethics Committee of Nanjing Agricultural University, Nanjing, China (No. PZW2022054).

Establishment of a model for rats with loss of sensory nerve

Fresh capsaicin was prepared at a concentration of 12.5mg/mL in a solution of tween-80, anhydrous ethanol, and physiological saline at a ratio of 1:1:8, with ultrasonic shaking until complete dissolution. Capsaicin was injected (0.1 mL/100 g) subcutaneously into the back of the neck. After the injection, the needle remained in the skin for 60 seconds to ensure the infusion did not reflux out of the syringe. The capsaicin treatment was administered for three consecutive days (30 mg/kg on day 1, 50 mg/kg on day 2, and 70 mg/kg on day 3).^{46,47} To prevent pulmonary edema after capsaicin injection, water was withheld for 6 hours before capsaicin injection. The needle-prick test was used after capsaicin injection to examine whether the model was successfully established.

Establishment of a model for rats with inferior alveolar nerve injury

After inhalation of anesthesia with isoflurane, there was no respiratory or circulatory system suppression. The surgical site in the right mandible was prepared and disinfected. A surgical incision parallel to the inferior margin of the mandible, approximately 1.5 mm long, was made approximately 5 mm below the mandibular angle. Muscles were bluntly separated along the inside of the mandible until the bone surface was reached. After reaching the inner surface of the mandible, the muscles were bluntly separated backward and inward to the mandibular foramen. The inferior alveolar nerve was cut to approximately 5 mm to prevent self-repair. The surgical site was then thoroughly rinsed with 0.9% physiological saline and the muscles and skin were sutured in layers. Antibiotics were administered by subcutaneous injection for three consecutive days after surgery. After anesthesia, place the rats from the sham surgery group on the operating table. After disinfection of the surgical area in the right mandible of rats, make a 1.5mm surgical incision approximately five millimeters below the mandibular angle parallel to the inferior border of the mandible. Subsequently, bluntly dissect the muscle until the bone surface is reached, exposing the inferior alveolar nerve without severing it, followed by wound irrigation and suturing.

METHOD DETAILS

Histology and immunohistochemical analysis of incisor

The mandibles of each group were fixed with 4% neutral paraformaldehyde for 24 hours, decalcified with 10% EDTA for 8 weeks, dehydrated and embedded in paraffin. The sections were stained with routine H&E and Masson's trichrome. Immunohistochemical staining was performed to detect the protein expression levels of β -catenin (1:100), CaMK-II (1:300) and Ror2 (1:50). After scanning the sections with the PANNORAMIC MIDI (3DHISTECH Ltd, Budapest, Hungary), Case Viewer software (3DHISTECH Ltd, Hungary) was used for visualization and analysis.

Immunofluorescence analysis

The expression of amelogenesis-related proteins, PGP9.5 (1:500), CGRP (1:400), Wnt5a (1:100), Amelx (1:100) and KLK4 (1:100) were detected using immunofluorescence staining. Briefly, after antigen retrieval and blocking, sections were incubated with primary antibodies overnight at 4°C. Secondary antibodies were conjugated to CoraLite488-conjugated Goat Anti-Rabbit IgG (1:200), CoraLite594-conjugated Goat Anti-Rabbit IgG (H + L) (1:200) and CoraLite594-conjugated Goat Anti-Mouse IgG (1:200). Then, the cell nuclei were stained with 4'-6-diamidino-2-phenylindole. The images were captured using a confocal laser microscope (Nikon Instruments Co., Inc., Japan).

Micro-computed tomography analysis

All rat incisors were scanned using micro-CT with a voxel resolution of 18 μ m (Bruker micro-CT, Belgium). The data were imported into DataViewer software (Bruker, Belgium) for analysis and reconstruction of the incisors. Simultaneously, the enamel thickness of the different incisors was measured.

mRNA sequencing analysis

mRNA sequencing was used to detect differences in incisor mRNA expression between the IAN and sham-operated groups. TRIzol reagent was used to extract RNA from the cervical loop of the lower incisors of the rats according to the instructions. RNA purity and quantity were determined using a NanoDrop 2000 spectrophotometer (Thermo Scientific, USA), and RNA integrity was evaluated using an Agilent 2100 Bioanalyzer (Agilent Technologies, Santa Clara, USA). The VAHTS Universal V5 RNA-seq Library Prep kit was used to construct a transcriptome library according to the instructions. Transcriptome sequencing and analysis were performed by OE Biotech Co., Ltd. (Shanghai, China). Differential gene expression analysis was carried out using DESeq2 software, where genes with a q-value <0.05, fold change >2, fold change <0.5

were defined as differentially expressed genes (DEGs). Subsequently, enrichment analysis using the hypergeometric distribution algorithm was conducted on the DEGs for the GO, KEGG, Reactome, and Wiki pathways to screen for significantly enriched functional entries.

Hard tissue sectioning assay

After fixing the incisor of rats in both the IAN and sham-operated groups with 4% paraformaldehyde for 48 h, the tissues were dehydrated and embedded in a light-curing monomer resin. Tissue sections were prepared using an EKAKT E300 sectioning and grinding system (Ekakt, Germany) and H&E. The examination and photography were performed using a transmitted light microscope (Zeiss AxioScope 2 plus; Carl Zeiss, Germany).

Scanning electron microscopy

To completely remove surface debris and broken minerals from the samples during preparation, the sagittal section of the incisors of the IAN and sham-operated groups were etched with 37% phosphoric acid for 20 s. After rinsing with distilled water, samples were ultrasonically cleaned thrice for 10 min each and stored in anhydrous ethanol before being removed and dried before testing. A 30 nm gold-palladium sputtering coating was applied, and the surface morphology of the sample was observed using a scanning electron microscope (S-3400N, Hitachi, Japan). SEM images were obtained to observe the surface morphology of the enamel.

Vickers hardness testing

The incisors of rats in the IAN and sham-operated groups were extracted. After cleaning, the tooth surfaces were embedded in a self-curing resin material, with the incisor lip exposed. The prepared specimens were placed on the testing table of an HV-1000 microhardness tester (Yanrun, China). The Vickers hardness mode was adjusted and the parameters were set as a load of 2.9421N and time of 10 s in atmospheric and room temperature testing environment. The Vickers surface microhardness of each specimen was measured. The surface hardness values of each specimen within the five regions (upper left, upper right, lower left, lower right, middle) were determined, and the average value was taken as the average Vickers hardness of the specimen.

Quantitative real-time PCR (qPCR) of gene expression in the cervical loop region of rat incisors

Total RNA from the rat incisor cervical loop tissue was extracted using the RNA Easy Fast Tissue Kit (TIANGEN, China). After measuring RNA concentration with the Nanodrop One (Thermo Fisher Scientific, USA), cDNA was synthesized using a reverse transcription kit (Vazyme, China). Subsequently, gene expression of genes related to rat incisor cervical loop tissue was evaluated using RT-qPCR on the 7300 Sequence Detection System (Applied Biosystems, USA). The primer sequences are listed in [Table S1](#).

QUANTIFICATION AND STATISTICAL ANALYSIS

The experimental data were statistically analyzed using GraphPad 8.0. The data was tested for normality and homogeneity of variances through Shapiro-Wilk test and Kolmogorov-Smirnov test. If it does follow a normal distribution, an independent sample t test is used to comparison between two groups, while one-way ANOVA was used to analyze comparisons among multiple groups. If the data does not conform to a normal distribution, the Kruskal-Wallis test is employed. Each group consisted of more than three rats. Differences were considered statistically significant at $p < 0.05$.